NUCLEIC ACIDS, PROTEIN SYNTHESIS, AND MOLECULAR GENETICS:

Stabilization of the MDM2 Oncoprotein by Interaction with the Structurally Related MDMX Protein

Darcie A. Sharp, Stephen A. Kratowicz, Michael J. Sank and Donna L. George

J. Biol. Chem. 1999, 274:38189-38196.
doi: 10.1074/jbc.274.53.38189

THE JOURNAL OF BIOLOGICAL CHEMISTRY
Vol. 274, No. 53, Issue of December 31, pp. 38189–38196, 1999
Printed in U.S.A.

Stabilization of the MDM2 Oncoprotein by Interaction with the Structurally Related MDMX Protein*

(Received for publication, June 9, 1999, and in revised form, September 10, 1999)

Darcie A. Sharp, Stephen A. Kratowicz, Michael J. Sank, and Donna L. George‡

From the Department of Genetics, University of Pennsylvania School of Medicine, Philadelphia, Pennsylvania 19104-6069

The MDM2 oncoprotein has transforming potential that can be activated by overexpression, and it represents a critical regulator of the p53 tumor suppressor protein. To identify other factors with a potential role in influencing the expression and/or function of MDM2, we utilized a yeast two-hybrid screening protocol. Here we report that MDM2 physically interacts with a structurally related protein termed MDMX. The results obtained in these studies provide evidence that C-terminal RING finger domains, contained within both of these proteins, play an important role in mediating the association between MDM2 and MDMX. The interaction of these proteins interferes with MDM2 degradation, leading to an increase in the steady-state levels of MDM2. MDMX also inhibits MDM2-mediated p53 degradation, with subsequent accumulation of p53. Taken together, these data indicate that MDMX has the potential to regulate the expression and function of the MDM2 oncoprotein.

An accumulating number of observations have implicated aberrant expression of the *MDM2* oncogene in the pathogenesis of human neoplasias. This mammalian gene has transforming potential that can be activated by overexpression (1, 2). Originally identified as a gene amplified and overexpressed in a spontaneously transformed mouse 3T3 cell line (3), *MDM2* is now known to be amplified in a variety of human tumors, particularly soft tissue sarcomas (4–7). Additionally, there are several cases reported of tumor cells having an elevated expression of MDM2 that results from mechanisms other than gene amplification, including enhanced translation of *MDM2* transcripts (8–10).

The *MDM2* gene encodes a key negative regulator of the p53 tumor suppressor protein, and the role of MDM2 overexpression in cell transformation has been attributed, at least in part, to its disruption of the biological activities of p53 (11, 12). MDM2 tightly associates with the N-terminal region of the p53 protein, inhibiting the trans-activation and G_1 growth arrest functions of p53 (13–16). Moreover, binding of MDM2 targets p53 for rapid degradation via the ubiquitin-proteasome pathway (17, 18). In recent reports, evidence has been obtained suggesting that MDM2 can function as an E3[1] ubiquitin ligase and is responsible for targeting both itself, and p53, for degradation (19, 20). Interestingly, the *MDM2* gene itself is a transcriptional target of p53. When activated as a transcription factor, p53 binds to a promoter region within the first intron of the *MDM2* gene and up-regulates its expression (21–24). Thus, there is evidence for an autoregulatory feedback loop involving the expression and function of *MDM2* and *p53* (23). Although the best characterized activities of MDM2 concern its functional interactions with p53, MDM2 also associates with other proteins. Some of these include E2F1 (25), pRb (26), and p300 (27). Such interactions could contribute to the transforming potential of MDM2 or may be concerned with modulating MDM2 function. Recently, a link between MDM2 and yet another tumor suppressor protein, $p14^{ARF}$ ($p19^{ARF}$ in mouse) was identified. An important consequence of complex formation with $p14^{ARF}$ is an abrogation of the ability of MDM2 to mediate p53 degradation and to inhibit the trans-activation function of p53 (28–30).

As illustrated by such examples, the identification of novel MDM2-interacting proteins would be expected to offer new clues to understand better the biological activities and/or regulation of the MDM2 oncoprotein. Toward that goal, we sought to identify cellular proteins that physically associate with MDM2. In initiating these studies, we noted that MDM2 contains several conserved structural motifs that likely are important for its biological activities (1). In addition to the N-terminal p53-binding domain, MDM2 has a central acidic domain, a putative nuclear localization signal, and a nuclear export signal. The C-terminal region of the MDM2 protein contains two cysteine-rich elements, classified as a C4 zinc finger domain and a C3HC4 RING finger (31). Recent investigations directly implicate certain zinc finger and RING finger domains in mediating protein-protein interactions or the formation of multiprotein complexes (32, 33). To test whether the C-terminal segment of the MDM2 protein, comprising the zinc finger and RING finger motifs, also might participate in complex formation with other proteins, we carried out a yeast two-hybrid screening assay.

As described in this report, we have identified an interaction between MDM2 and a structurally related protein, MDMX (34, 35). Our data indicate that the RING finger domains contained within both of these proteins are necessary to mediate this interaction. Notably, complex formation between MDM2 and MDMX leads to a stabilization of MDM2, resulting in an elevation of steady-state levels of MDM2 protein. MDMX also interferes with MDM2-mediated degradation of p53, resulting in an increase in p53 protein levels. The data presented here suggest a role for MDMX in the regulation of MDM2 expression and have implications for understanding the cellular functions of the MDM2 oncoprotein.

* This work was supported by United States Public Health Service Grant CA-66741 from the NCI of the National Institutes of Health. The costs of publication of this article were defrayed in part by the payment of page charges. This article must therefore be hereby marked "*advertisement*" in accordance with 18 U.S.C. Section 1734 solely to indicate this fact.

‡To whom correspondence should be addressed: Dept. of Genetics, University of Pennsylvania School of Medicine, 713 Stellar-Chance Bldg., 422 Curie Blvd., Philadelphia, PA 19104-6069. Tel.: 215-898-5032; Fax: 215-573-9411; E-mail: georged@mail.med.upenn.edu.

[1] The abbreviations used are: E3, ubiquitin-protein isopeptide ligase; aa, amino acids; IP, immunoprecipitation; PCR, polymerase chain reaction; PAGE, polyacrylamide gel electrophoresis; X-gal, 5-bromo-4-chloro-3-indolyl β-D-galactopyranoside; AD, activation domain; BD, binding domain.

EXPERIMENTAL PROCEDURES

Yeast Two-hybrid Screen—A DNA fragment encoding the C-terminal 215 amino acid (aa) residues of human MDM2 was fused in-frame with the yeast GAL4 DNA binding domain in the pBD-GAL4 Cam phagemid vector (Stratagene) to create the hybrid bait protein. A randomly primed cDNA library was constructed in the pAD-GAL4 phagemid (Stratagene) using poly(A)$^+$ RNA isolated from human thymus (CLONTECH). The bait and target plasmids were co-transformed into YRG-2 yeast cells. Colonies with plasmid DNA encoding target proteins that interact with the bait protein are identified by transcription of the *HIS3* and *lacZ* reporter genes integrated into the genome of the yeast host. Approximately 3×10^6 transformants were screened for colonies that would grow on media lacking tryptophan (Trp), leucine (Leu), and histidine (His). To confirm the presence of interacting proteins, positive transformants were assayed for expression of the *lacZ* reporter gene using an X-gal filter assay for detection of β-galactosidase activity. Typically, blue coloration of colonies appeared within 1–3 h of incubation of the filter in the *lacZ*/X-gal buffer at 30 °C. To verify further protein-protein interactions, plasmid DNA was rescued from positive colonies and re-transformed into YRG-2 yeast cells with the MDM2 bait plasmid. Nucleotide sequence analysis was carried out to characterize the target DNA of positive colonies.

Plasmid Constructs and Antibodies—A full-length human *MDMX* cDNA fragment encoding aa 1–490 was generated by a random hexamer-primed reverse transcription reaction using human kidney RNA (CLONTECH) followed by PCR using forward and reverse primers containing the first and last coding triplets of the human *MDMX* cDNA. All nucleotide and aa sequence numbers for *MDMX* primer design relate to the first ATG coding triplet as number 1 (35). The 5′ primer included an *Xho*I site, and the 3′ primer included a *Bam*HI site for subsequent cloning reactions. This PCR product was cloned into the TOPO PCR 2.1 vector (Invitrogen) to generate the *MDMX* plasmid termed pCK4; the DNA sequence was verified, and this clone was used as a template to generate additional *MDMX* constructs, as described below. DNA fragments encoding full-length *MDMX* and *MDMX* lacking the C-terminal 59 aa (MDMX without RING) were both cloned into the yeast phagemid vector pAD-GAL4 by including into the oligonucleotide primers 5′ *Srf*I and 3′ *Sal*I restriction sites. The 5′ and 3′ primers for the full-length *MDMX* construct included sequences representing the first ATG codon and last (stop) codon, respectively. For the MDMX without RING construct, the 5′ primer included sequences for the first ATG codon, and the 3′ primer included *MDMX* coding sequence up to base pair 1290. For the MDMX-(101–490)-Myc construct, the 5′ primer included the sequences for an internal ATG at aa residue 101, and the 3′ primer included the last (stop) codon of the MDMX cDNA. To generate the *MDMX* mammalian expression plasmid MDMX-Myc, a C-terminal Myc epitope tag was added to the *MDMX* coding sequence by using a *Bam*HI-*Xho*I restriction digest to release the insert from plasmid pCK4; the released insert was subcloned into the pcDNA 3.1(−)Myc His A mammalian expression vector (Invitrogen). An N-terminally Myc-tagged *MDMX* construct was constructed by introducing the sequence of a Myc epitope (5′ GAGGAGCAGAAGTTGATCTCCGAGGAG-GATCTCCTC 3′) into the *Hin*dIII-*Bam*HI site of the pcDNA 3.1(+) vector (Invitrogen). The full coding region and stop codon of the human *MDMX* gene was generated by reverse transcriptase-PCR reactions using human kidney RNA. The 5′ primer included a *Bam*HI site, and the 3′ primer included an *Xho*I site to facilitate cloning the *MDMX* sequence in-frame with the Myc tag in the pcDNA 3.1(+) vector. A FLAG epitope tag (5′ CCTGTCATCGTCGTCCTTGTAGTC 3′) was added to the C terminus of *MDMX* by PCR of the *MDMX* construct pCK4, using 5′ and 3′ PCR primers that included a *Bam*HI restriction site. The PCR product was cloned into the *Bam*HI site of the mammalian expression vector CMV-NeoBam. The MDMX-(1–153)-Myc construct was generated by *Xho*I-*Eco*RV digestion of the MDMX-Myc plasmid; the *MDMX* insert DNA fragment was reinserted directionally into the *Xho*I-*Eco*RV site of pcDNA 3.1(−)Myc His A. The MDMX-(1–392)-Myc construct was generated by *Eco*RI digestion of pCK4; the *MDMX* insert DNA fragment was reinserted into the *Eco*RI site of pcDNA 3.1(−)Myc His B (Invitrogen).

The S-*MDM2* and p53-SN3 constructs in the CMV-NeoBam mammalian expression vector have been described previously (8, 9). The *MDM2*, pBD-GAL4 yeast two-hybrid plasmids termed MDM2 full, MR1, MR2, and MDM2 without p53, were all generated by PCR using the human S-*MDM2* construct as a template. The 5′ and 3′ primers included an *Eco*RI site and *Srf*I site, respectively, to facilitate cloning into the yeast pBD-GAL4 vector. The *MDM2* sequences within the 5′ PCR primers for MDM2 without p53, MR1, and MR2 started at base pair 306, 828, and 1047, respectively, to generate these N-terminally truncated forms of MDM2. In each case, the 3′ primer included the *MDM2* stop codon. The *MDM2* without RING yeast plasmid construct was generated by *Sal*I digestion of the MDM2 full plasmid; the digest product was then self-ligated following gel purification. Point mutants of *MDM2* or *MDMX* were generated using the Altered Sites II *in vitro* mutagenesis system (Promega).

Monoclonal antibodies anti-MDM2 IF2 and anti-p53 DO-1 were obtained from Calbiochem. Anti-MDM2 monoclonal antibody 2A10 was a kind gift from Dr. Arnold Levine. Monoclonal antibody anti-Myc 9E10 and rabbit polyclonal antibody to p53 (p53fl393) were obtained from Santa Cruz Biotechnology or from Calbiochem. Anti-FLAG M2 and anti-β-actin AC-15 were obtained from Sigma.

In Vitro Binding Assays—MDM2 and MDMX-Myc expression constructs were individually transcribed and translated in the presence or absence of [^{35}S]methionine using the T7-coupled reticulocyte lysate system (TNT; Promega). Following a 2-h incubation at 30 °C, the protein synthesis inhibitor cycloheximide was added to the reactions (100 μg/ml final concentration) that were then incubated for an additional 10 min at room temperature. MDM2 and MDMX-Myc *in vitro* translation products were combined together and incubated for 30 min at 30 °C. Following the addition of 450 μl of dilution buffer (0.5% Nonidet P-40, 150 mM NaCl, 50 mM Tris-Cl, pH 8, 5 mM EDTA) and 1–3 μg of the appropriate antibodies to each binding reaction, the samples were incubated for 1 h at 4 °C with mixing. To isolate immunocomplexes, 30 μl of a protein A/protein G-agarose bead mix (Life Technologies, Inc.) was added, and reactions were incubated for another 30 min at 4 °C with mixing. Following this incubation, the beads were pelleted by centrifugation, washed three times in washing buffer (0.7 M NaCl, 0.5% Nonidet P-40, 5 mM EDTA, pH 8, 50 mM Tris-Cl, pH 8), and one time in phosphate-buffered saline. After washing, pelleted beads were resuspended in 50 μl of SDS sample loading buffer and boiled 5 min. Denatured proteins released into the supernatant were resolved by SDS-10% polyacrylamide gel electrophoresis (PAGE) and visualized by exposure to x-ray film after fluorography.

Cell Culture, DNA Transfections, and RNA Blot Analysis—H1299 lung adenocarcinoma cells (p53 null) and JEG-3 choriocarcinoma cells (wild-type p53) were maintained in Dulbecco's modified Eagle's medium supplemented with 10% fetal bovine serum and antibiotics. H1299 cell transfections were carried out using the Lipotaxi reagent according to guidelines of the manufacturer (Stratagene) or by a standard calcium phosphate precipitation protocol. In all transfections the total amount of each vector was equalized, as was the total amount of DNA. Approximately 24–48 h post-transfection, the cells were harvested and lysed (1% Nonidet P-40, 250 mM NaCl, 5 mM EDTA, 50 mM Tris-Cl, pH 7.4, supplemented with the protease inhibitors aprotinin and leupeptin). DNA was transfected into JEG-3 cells using the calcium phosphate precipitation protocol. At 48 h post-transfection, the cells were harvested and lysed. To examine the relative stability of MDM2 protein, H1299 cells were transfected as described above. At 48 h post-transfection, fresh media containing cycloheximide (75 μg/ml final concentration) were added. The cells were harvested at various time points, and cell lysates were subjected to Western blot analysis.

For Northern blot analysis, total cellular RNA from transfected H1299 cells was isolated using RNA Isolator (Genosys). Samples (10 μg) were resolved on formaldehyde-agarose gels and transferred to nitrocellulose as described previously (36). Probes were radiolabeled with ^{32}P using random primers (Prime-It-II, Stratagene).

Immunoprecipitation and Western Blot Analysis—For immunoprecipitation assays, cell lysates (approximately 1–3 mg of protein) were incubated with 1–3 μg of the appropriate antibody and lysis buffer (final volume, 500 μl) for 1 h at 4 °C with mixing. Following the addition of 40 μl of a protein A/protein G-agarose bead mix, the reactions were incubated for 30 min at 4 °C with mixing. The beads were washed twice in RIPA buffer (1% Triton X-100, 150 mM NaCl, 50 mM Tris-Cl, pH 7.4, 0.1% SDS, 1% sodium deoxycholate), resuspended in 50 μl of SDS sample loading buffer, and boiled for 5 min. The immunoprecipitates were separated by SDS-PAGE and transferred to nitrocellulose membranes (Schleicher & Schuell). For immunoblotting experiments, 50–75-μg samples of total cellular lysate in SDS loading buffer were separated by 7.5–10% SDS-PAGE. Western blot analysis was performed using an enhanced chemiluminescence system (ECL, Amersham Pharmacia Biotech).

RESULTS

Yeast Two-hybrid Analysis Identifies MDMX as an MDM2-binding Protein—To identify cellular proteins that interact

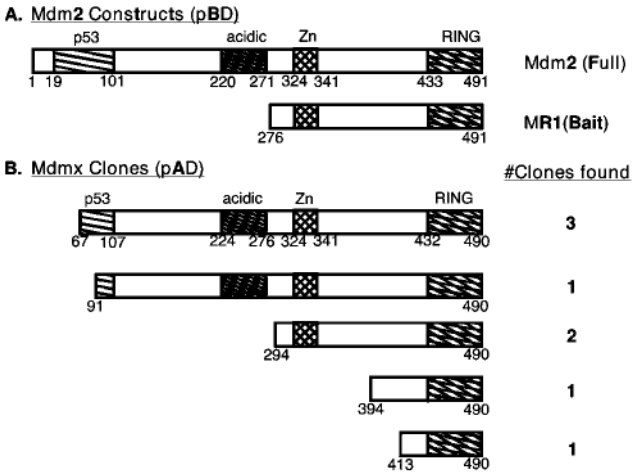

FIG. 1. **Human MDMX binds MDM2.** *A,* schematic illustration of full-length human MDM2 protein (491 aa). Indicated are relative positions of amino acid residues encoding the p53-binding domain (*p53*), acidic domain, zinc finger domain (*Zn*), and RING finger domain (*RING*). A DNA fragment encoding the C-terminal 215 aa residues of MDM2 (termed MR1) was fused in-frame with the yeast Gal4 DNA binding domain (Gal4-BD) and used as "bait" to screen for MDM2-interacting proteins in a yeast two-hybrid assay. *B*, schematic illustration of five independent clones rescued from colonies scored positive for interaction between the MDM2 bait (MR1) and the yeast library "prey" plasmids. Two of the cDNAs illustrated were isolated more than once, as indicated by the number of clones found. Nucleotide sequence analysis and search of DNA data bases revealed that all of these cDNAs were derived from overlapping regions of the human *MDMX* gene. A schematic illustration of notable structural features of the MDMX protein (490 aa) is shown and includes the p53 binding domain (*p53*), acidic domain, zinc finger domain (*Zn*), and RING finger domain (*RING*).

with MDM2, a yeast two-hybrid screen was employed. The C-terminal 215 aa of MDM2, including the zinc finger region and the RING finger domain, were fused to the GAL4 DNA-binding domain (BD). As detailed under "Experimental Procedures," this construct was used as bait to screen a randomly primed human thymus cDNA library that was fused to the GAL4 transcriptional activation domain (AD) (Fig. 1*A*). From a screen of approximately 3×10^6 yeast transformants, 47 colonies scored as positive for reporter gene activity (His^+LacZ^+). Of these, the first eight were chosen for further analysis; all scored positive in secondary screening assays, indicating an interaction with the GAL4 BD-MDM2 fusion protein. DNA sequence analysis revealed that each of the rescued cDNAs from the positive clones were derived from the human *MDMX* gene (Fig. 1*B*). The remaining 39 His^+LacZ^+ colonies all hybridized positively to a radioactively labeled *MDMX* probe in colony-lift assays.

The MDMX protein was identified in a screen for proteins that bind to the tumor suppressor p53 (34, 35). Interestingly, it exhibits high structural homology to MDM2. Overall, MDM2 and MDMX exhibit 32.6% amino acid sequence identity; the greatest conservation resides within the N-terminal (50.5%) and C-terminal (31.4%) portions of the two proteins. The N-terminal regions include the p53-binding domains, and the C-terminal regions of these proteins contain the putative metal-binding, zinc finger, and RING finger, domains. As indicated by the results of our yeast two-hybrid screen (Fig. 1), the C-terminal regions of the MDM2 and MDMX proteins likely play an important role in their interaction. In particular, a polypeptide containing only the last 77 aa residues of MDMX, which includes the RING domain, is capable of interaction with MDM2 (Fig. 1*B*). For MDM2, a slightly larger polypeptide that includes both the zinc finger and RING finger domains (aa 276–491) is required for interaction with MDMX (Fig. 1*A* and Fig. 2*A*).

The yeast two-hybrid assays were extended to test further the importance of the C-terminal protein domains in the MDMX-MDM2 interaction. The results (Fig. 2) demonstrated that full-length versions of the MDM2 and MDMX proteins can interact in yeast cells. In addition, deletion of the N-terminal p53-binding region, or the central acidic domain, of MDM2 did not interfere with MDM2-MDMX interactions. However, a truncated MDM2 protein, lacking the C-terminal 49 aa residues, failed to interact with MDMX (Fig. 2*A*). Deletion of the C-terminal 59 aa residues of MDMX also resulted in a loss of interaction of the two proteins.

Evidence suggests that the C-terminal region of MDM2 binds two molecules of zinc in an interleaved fashion (37). To examine more specifically the role of the RING domain in MDM2-MDMX interaction**,** we therefore introduced mutations at conserved cysteine residues implicated in this metal ligation. MDM2 proteins containing a single mutation (C441G or C478R) or a double mutation (C438G,C441G or C475Y,C478R) within the RING domain failed to interact with MDMX (Fig. 2*A*). Mutation of a threonine residue (T455A) that is located within the RING domain, but does not seem to be involved in metal ligation (37), did not disrupt the ability of MDM2 and MDMX to associate (Fig. 2*A*). The introduction of either a single mutation (C437G) or a double mutation (C437G,C440G) within the RING domain of MDMX also disrupted interaction with MDM2 (Fig. 2*B*). It should be noted that both MDM2 and MDMX proteins containing such point mutations, and those with the C-terminal deletions noted above, still retained the ability to associate with p53 protein in this yeast two-hybrid system (data not shown). Taken together, these results indicate that the RING finger domain of MDM2 is necessary for interaction with MDMX; in contrast, the RING domain of MDMX likely is both necessary and sufficient for binding to MDM2. Interestingly, we have found no evidence for homo-oligomerization of either the MDMX or MDM2 proteins (data not shown). This result lends additional support to the specificity of the RING-RING interaction between MDM2 and MDMX.

MDMX and MDM2 Associate in Vitro and in Vivo—The MDM2-MDMX interaction also was detected in a cell-free system. Full-length MDMX, containing a c-Myc epitope tag (MDMX-Myc), and full-length MDM2 were individually produced by translation in a rabbit reticulocyte lysate system. The MDMX and MDM2 proteins are very similar in size (85–95 kDa; Fig. 3, *lanes 1* and *2*). Thus, to ensure accurate identification of the proteins, co-immunoprecipitation reactions were carried out following the ^{35}S labeling of only one of the proteins per reaction. ^{35}S-Labeled MDMX-Myc protein was incubated with unlabeled MDM2 to allow complex formation, and the reactions were immunoprecipitated with anti-MDM2 antibody. The ^{35}S-labeled MDMX-Myc protein is clearly detectable in these immunocomplexes (Fig. 3, *lane 3*). Consistent results were obtained when ^{35}S-labeled MDM2 protein was incubated with unlabeled MDMX-Myc followed by immunoprecipitation with anti-Myc antibody; the presence of ^{35}S-labeled MDM2 in the immunoprecipitates is illustrated in Fig. 3, *lane 4.* In contrast, there was no evidence for cross-reaction between the anti-MDM2 antibody and MDMX-Myc (Fig. 3, *lane 5*) or between the anti-Myc antibody and MDM2 (Fig. 3, *lane 6*). These results suggest that MDM2 and MDMX interact directly.

MDM2-MDMX binding was assessed in mammalian cells following transient transfection analysis. Mammalian expression plasmids encoding either a Myc-tagged MDMX protein or MDM2 protein were transfected into H1299 human lung carcinoma cells, either separately or together. Cell extracts were analyzed by IP-Western blot analysis. For the co-transfected cells, immunoprecipitation with anti-MDM2 antibodies, fol-

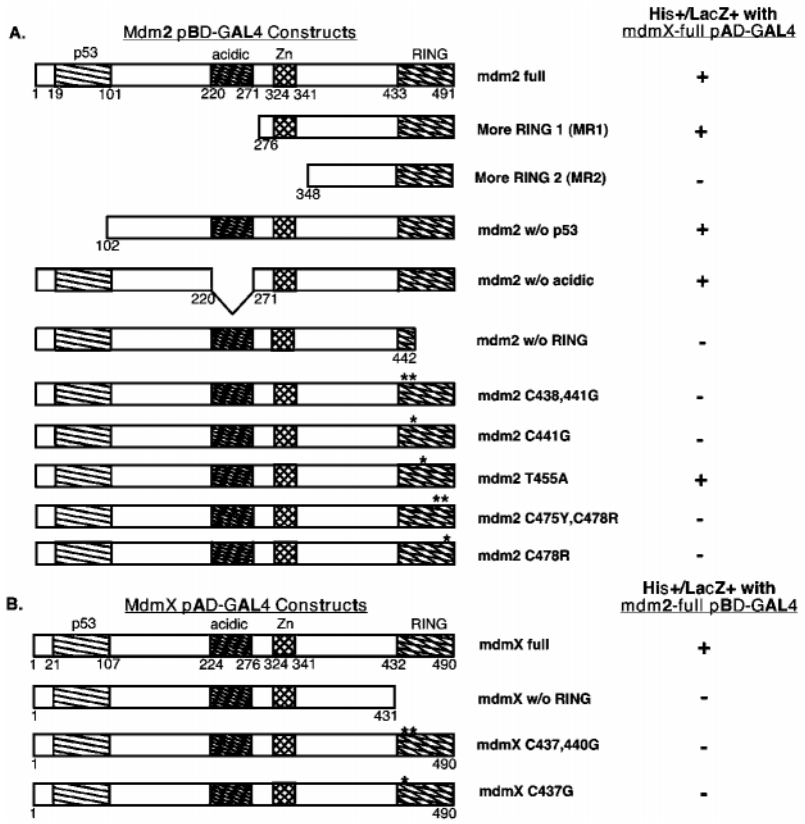

FIG. 2. **Yeast two-hybrid interaction between MDM2 and MDMX proteins.** Yeast strain YRG-2 was co-transformed with the indicated yeast expression plasmids and tested for positive two-hybrid interactions by growth of colonies on media lacking amino acids Trp, Leu, and His, followed by an assay for β-galactosidase activity ($His^+/LacZ^+$). *A,* DNA regions encoding full-length, deleted, or mutated versions of MDM2, as indicated by the schematic illustrations, were cloned in frame with the GAL4 DNA binding domain (*MDM2 pBD-GAL4 constructs*). Proteins encoded by these expression plasmids were tested for interaction with full-length MDMX cloned in frame with the GAL4 activation domain (*MDMX full pAD-GAL4* construct). *Asterisks* indicate positions of altered amino acids. *B,* DNA regions encoding full-length, deleted, or mutated versions of MDMX, as indicated, were cloned in frame with GAL4 activation domain (*MDMX pAD-GAL4 constructs*). Proteins encoded by these expression plasmids were tested for interaction with full-length MDM2 cloned in frame with the Gal4 DNA binding domain (*MDM2 pBD-GAL4* construct). *Asterisks* indicate positions of altered amino acids.

lowed by immunoblot analysis using an antibody to the Myc-epitope tag, identified MDMX-Myc bound to MDM2 (Fig. 4, *lane 1*). The MDMX-Myc protein was detected in these immunocomplexes when the cell lysates were immunoprecipitated using two different antibodies to MDM2 (2A10 and IF2), either together (Fig. 4, *lane 1*) or individually (data not shown). Similarly, when lysates from the co-transfected cells were immunoprecipitated with anti-Myc antibody, Western blot analysis consistently revealed the presence of MDM2 proteins in the immunocomplexes (Fig. 4, *lane 6*).

To examine the association of endogenous MDM2 with transfected MDMX protein, we repeated the IP-Western analyses using JEG-3 choriocarcinoma cells, which have elevated levels of endogenous MDM2 protein (8). The JEG-3 cells were transfected with either a Myc-tagged MDMX expression vector, a FLAG-tagged MDMX expression vector, or with empty vector. Cell lysates were immunoprecipitated using anti-Myc antibody, anti-FLAG antibody, or a control antibody (anti-rabbit IgG). In these experiments, the interaction of MDMX with endogenous MDM2 was readily detectable. The endogenous MDM2 protein in the JEG-3 cells co-precipitated with MDMX-Myc using the anti-Myc antibody (Fig. 4*B, lane 1*) and with MDMX-FLAG using the anti-FLAG antibody (Fig. 4*B, lane 3*). In control assays where JEG-3 cells were transfected with empty vector alone, MDM2 was not precipitated using anti-Myc, anti-FLAG, or anti-rabbit IgG antibodies (Fig. 4*B, lanes 5–7*). In summary, these data demonstrate that the MDM2 and MDMX proteins can interact in mammalian cells.

MDMX Increases the Steady-state Level of MDM2—During the course of these studies, we noted that co-transfection of the *MDM2* and *MDMX-myc* expression plasmids resulted in a reproducible and significant increase in the steady-state level of MDM2 protein. An example of this can be seen in Fig. 4*A* (compare *lanes 8* and *9*). This result suggested that MDMX may be modulating MDM2 expression. To assess further this possibility, H1299 cells were co-transfected with a constant amount of *MDM2* plasmid and increasing amounts of *MDMX-myc* plasmid. Steady-state MDM2 protein levels in the transfected cells were examined by Western blotting. The results demonstrate that increased MDMX-Myc protein expression is accompanied by a dose-dependent increase in the steady-state levels of MDM2 protein (Fig. 5*A*). Expression of the transfected *MDMX-myc* construct in these cells was confirmed by Western blotting (data not shown).

Interestingly, MDMX protein levels were not obviously affected by co-expression of MDM2 (Fig. 4*A*, compare *lanes 4* and *5*). To confirm this, H1299 cells were co-transfected with a constant amount of plasmid for FLAG-tagged MDMX and with increasing amounts of *MDM2* plasmid. We carried out these transfections at higher *MDM2:MDMX* plasmid ratios (1:1 and 5:1) than previously utilized, to ensure that adequate levels of MDM2 would be present to test any effects it might have on MDMX levels. Cell lysates were analyzed for steady-state MDMX protein levels by Western blotting using anti-FLAG antibody. The results obtained from this experiment were consistent with previous data, indicating that that co-expression of MDM2 has no discernible effect on the steady-state levels of MDMX protein (Fig. 5*B*). Expression of the transfected *MDM2* construct in the transfected cells was confirmed by Western blotting (data not shown).

Northern blot assays demonstrated that *MDM2* mRNA levels were not different in the presence of MDMX (Fig. 5*C*). It is likely, therefore, that the increase in MDM2 is mediated by a change in the half-life of the protein. To test this, we examined the relative stability of MDM2 in the presence or absence of MDMX. For these assays, cellular protein synthesis was inhibited by the addition of cycloheximide, and the abundance of MDM2 protein was examined by Western blotting. We determined that under these experimental conditions, the initial half-life of transfected MDM2 in the H1299 cells is approximately 30 min (Fig. 5*D, lanes 1–4*); this value is consistent with previous estimates of the half-life of endogenous MDM2 (15–30

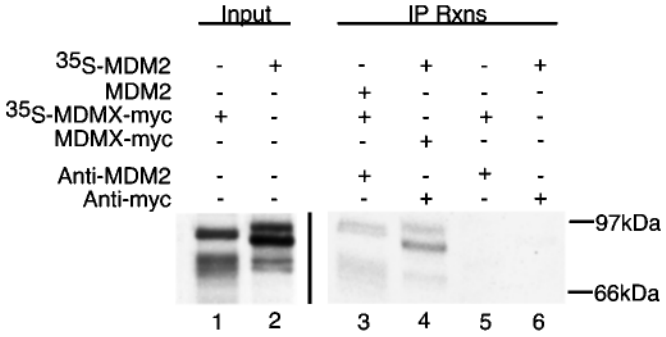

FIG. 3. **MDM2 and MDMX proteins interact *in vitro*.** Full-length MDM2 and MDMX-Myc were produced in separate *in vitro* translation reactions in a rabbit reticulocyte system, either in the presence or absence of ^{35}S-labeled methionine. Samples were resolved by SDS-PAGE and visualized by x-ray film exposure following fluorography. Molecular masses of protein size markers are indicated. Aliquots of the individually translated, ^{35}S-labeled MDMX-Myc (*lane 1*) and ^{35}S-labeled MDM2 (*lane 2*) proteins are shown. ^{35}S-Labeled Myc-MDMX was incubated in the presence (*lane 3*) or absence (*lane 5*) of unlabeled MDM2, followed by precipitation with anti-MDM2 antibody. Similarly, ^{35}S-labeled MDM2 was incubated in the presence (*lane 4*) or absence (*lane 6*) of unlabeled MDMX-Myc, followed by precipitation with anti-Myc antibody. *Rxns,* reactions.

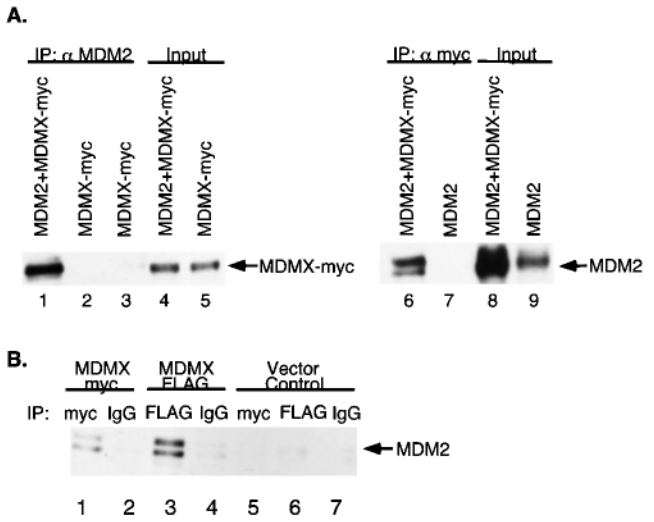

FIG. 4. **MDM2 and MDMX proteins associate *in vivo*.** *A,* expression plasmids encoding full-length MDM2 and MDMX-Myc proteins were transfected individually or together into H1299 cells as indicated, and cell lysates were analyzed using IP-Western blot protocols. A portion of the lysate was immunoprecipitated with anti-MDM2 monoclonal antibodies 2A10 and IF2, either together (*lane 1*), or separately (*lane 2*, 2A10; *lane 3*, IF2), or with anti-Myc monoclonal antibody 9E10 (*lanes 6* and *7*). Following SDS-PAGE separation, cell lysates and immunoprecipitates were analyzed by Western blotting carried out with anti-MDM2 (IF2) or anti-Myc (9E10) antibodies. A portion of the cell lysate (75 μg) was also loaded as a control (*lanes 4, 5, 8*, and *9*). Proteins were visualized using an enhanced chemiluminescence (ECL) detection system. *B,* JEG-3 cells were transfected with expression constructs encoding MDMX-Myc (*lanes 1* and *2*), MDMX-FLAG (*lanes 3* and *4*), or vector alone (*lanes 5–7*). Cell lysates were immunoprecipitated with anti-Myc antibody, anti-FLAG antibody, or with a nonspecific antisera (rabbit IgG), as indicated, followed by Western blot analysis for MDM2 protein (IF2 antibody).

min) as assayed by pulse-chase protocols (2, 8, 38). Co-expression of MDMX with MDM2, however, led to a substantial increase in the stability of the MDM2 protein, increasing the half-life of MDM2 to greater than 2 h (Fig. 5*D, lanes 5–8*). Although the use of cycloheximide to inhibit protein synthesis may allow only an estimate of protein half-life, it is clear from these studies that co-expression of MDMX results in a substantial increase in the stability of MDM2 protein.

Stabilization of MDM2 by MDMX Is Dependent on Protein-Protein Interaction—Experiments were carried out to test whether the increase in MDM2 protein by MDMX depends on a physical interaction between these proteins. Data obtained in our yeast two-hybrid analyses indicated that the C terminus of MDMX is important for its interaction with MDM2. Therefore, for these studies we utilized *MDMX* constructs encoding modified MDMX proteins, as follows: MDMX(C437G,C440G) protein contains mutations of two conserved cysteine residues at positions 437 and 440 within the RING domain; MDMX-(1–392) is missing the C-terminal 98 aa residues of the full-length MDMX protein, including the RING domain (432–490); MDMX-(1–153) encodes a more severely truncated MDMX protein containing only the first 153 aa residues. The protein encoded by MDMX-(1–153) is very similar in size to a recently identified *MDMX* product, termed MDMX-S ("short form"), which lacks the central and C-terminal portions of the full-length MDMX protein (39).[2]

H1299 cells were co-transfected with an *MDM2* expression plasmid and an expression plasmid encoding either full-length MDMX or a modified MDMX protein. All of these MDMX products contain a Myc epitope tag for protein detection. As expected, co-transfection of MDM2 with the MDMX-full construct led to an increase in the steady-state level of MDM2 protein (Fig. 6, *lanes 4* and *6*). In contrast, introduction of mutations within the RING finger, or truncation of the C-terminal 98 amino acids, abrogated the ability of MDMX to increase MDM2 levels (Fig. 6, *lanes 2, 3,* and *7*).

We examined the two, C-terminally truncated MDMX proteins in IP-Western blot analyses, and we found that they do not bind to MDM2 (Fig. 7, *lanes 2* and *3*). Failure of these truncated MDMX proteins to bind to MDM2 was not due to inadequate expression, since both the MDMX-(1–392) and the MDMX-(1–153) proteins were expressed at levels at least as high as the full-length MDMX protein (Fig. 7, *lanes 7–9*). Additionally, this IP-Western blot analysis confirmed that all three of these MDMX protein forms are able to bind to p53 protein (data not shown). The importance of the MDMX-MDM2 interaction for stabilization of MDM2 is again illustrated by comparing the steady-state MDM2 protein levels present in the input lysates for these IP-Western analyses (Fig. 7, *lanes 4–6*). In summary, these experiments demonstrate that stabilization of MDM2 by MDMX requires an interaction between these proteins.

Interaction of MDMX with MDM2 and p53—The MDMX protein contains the MDM2-binding domain at its C terminus and the p53-binding domain at its N terminus. This raises the possibility that MDMX may be able to form ternary complexes with MDM2 and p53. However, testing this idea is complicated by the ability of both MDMX and MDM2 to independently bind to p53. To approach this question, therefore, we constructed an N-terminally truncated MDMX mutant that is missing the first 100 amino acid residues. This mutant retains the C-terminal MDM2-binding region but lacks the p53 binding domain. We then asked whether a ternary complex could form, under conditions where MDM2 would serve as a "bridging" partner for p53 and the MDMX-(101–490) protein. Control IP-Western blot analysis of transfected cells confirmed that the N-terminally truncated MDMX-(101–490) protein interacts well with MDM2 (*lane 2*) but is impaired in its ability to bind to p53 (*lane 3*). For cells transfected with expression constructs for all three proteins, IP-Western blot analysis revealed the presence of MDMX-(101–490), as well as MDM2, in the p53 immunocomplexes (Fig. 8, *lane 5*). These results indicate that MDMX,

[2] D. A. Sharp, S. A. Kratowicz, M. J. Sank, and D. L. George, unpublished results.

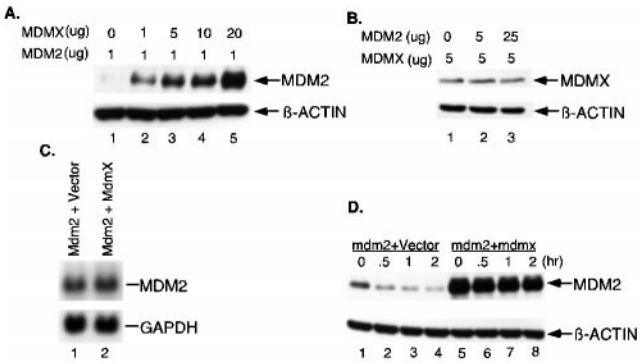

FIG. 5. **MDMX increases the steady-state level of MDM2 protein and MDM2 protein stability but does not alter MDM2 RNA levels.** *A,* for Western blot analysis, H1299 cells were co-transfected with an *MDM2* plasmid (1 μg) and with increasing amounts of an *MDMX-myc* plasmid (0–20 μg). Vector plasmid was added to maintain equivalent plasmid DNA concentrations in each transfection. Total cell lysates were subjected to Western blot analysis using anti-MDM2 monoclonal antibody (IF2). Equal loading of cell lysates was confirmed by probing the same blot with an anti-β-actin antibody. *B,* H1299 cells were co-transfected with an *MDMX-myc* plasmid (5 μg) and increasing amounts of an *MDM2* plasmid (0–25 μg). Total cell lysates were subjected to Western blot analysis using anti-Myc antibody (9E10). Equal loading of cell lysates was confirmed by probing the same blot with an anti-β-actin antibody. *C,* for RNA blot analysis, H1299 cells were transfected with 1 μg of the *MDM2* plasmid and 10 μg of either the empty vector (*lane 1*) or the *MDMX-myc* plasmid (*lane 2*). Total RNA was isolated 48 h later, and 10 μg of each sample was analyzed by Northern blotting. The RNA blot was hybridized sequentially with probes for MDM2 and a loading control, glyceraldehyde-3-phosphate dehydrogenase (*GAPDH*). *D,* MDMX increases MDM2 protein stability. H1299 cells were co-transfected with an *MDM2* plasmid (4 μg) together with either empty vector (20 μg) or with *MDMX-myc* plasmid (20 μg). 48 h later, the cells were treated with the protein synthesis inhibitor cycloheximide for the periods indicated. Cell lysates were subjected to Western blot analysis with anti-MDM2 antibody (IF2). Equal protein loading was confirmed by probing the same blot with anti-β-actin antibody.

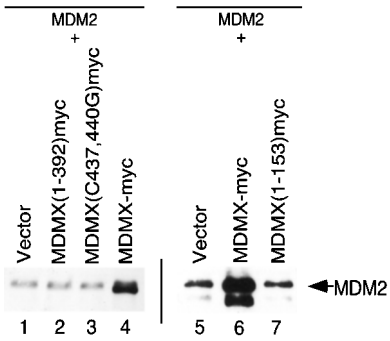

FIG. 6. **Mutation or deletion of the C-terminal region of MDMX abrogates its ability to stabilize MDM2.** Western blot analysis of MDM2 expression in H1299 cells co-transfected with expression plasmids encoding MDM2 and either vector alone (*lanes 1* and *5*), full-length MDMX (*lanes 4* and *6*), C-terminally truncated MDMX (aa 1–153) (*lane 7*), C-terminally truncated MDMX (aa 1–392) (*lane 2*), or MDMX (C437G,C440G) (*lane 3*) with a double (cysteine to glycine) mutation in the RING domain at amino acid residues 437 and 440. The anti-MDM2 antibody used was IF2.

MDM2, and p53 are capable of forming a triple complex, with the potential to alter the expression and biological activity of the MDM2 and p53 proteins.

MDMX Inhibits MDM2-mediated p53 Degradation—MDM2 represents a key factor in the control of p53 turnover. Recent studies have shown that binding of MDM2 targets p53 for rapid degradation via the ubiquitin-proteasome pathway (17, 18) and that disruption of this pathway leads to an accumulation of p53 protein. Therefore, we investigated whether MDMX expression interferes with the ability of MDM2 to promote p53 degradation. Transient transfections were carried out using the p53-

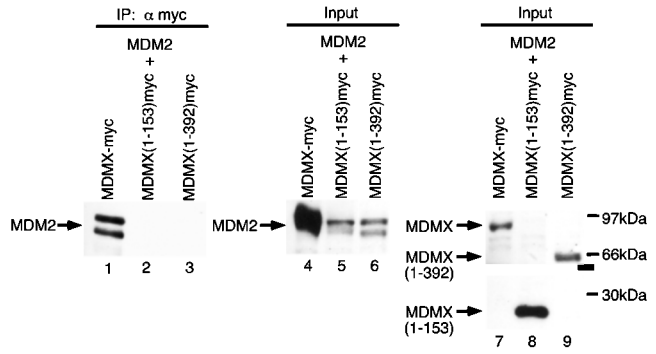

FIG. 7. **Stabilization of MDM2 by MDMX correlates with complex formation.** IP-Western blot analysis of H1299 cells co-transfected with expression plasmids encoding MDM2 and either full-length MDMX (*lane 1*), C-terminally truncated MDMX-(1–153) (*lane 2*), or C-terminally truncated MDMX-(1–392) (*lane 3*). Cell lysates were immunoprecipitated with anti-Myc antibody (9E10), followed by Western blot analysis for MDM2 protein (IF2 antibody). A portion (50 μg) of each cell lysate (*Input*) was also loaded as a control for expression of MDM2 (*lanes 4–6*) or MDMX proteins (*lanes 7–9*).

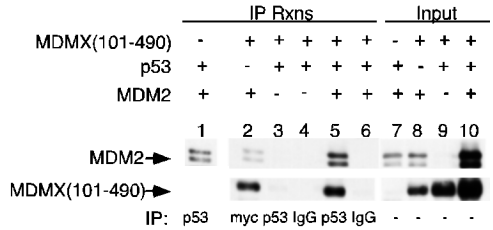

FIG. 8. **MDM2, p53, and MDMX-(101–490) form a triple complex.** IP-Western blot analysis of H1299 cell lysates following transient transfection with combinations of expression plasmids for MDM2, p53, or a N-terminally truncated, Myc-tagged MDMX-(101–490) protein. Cell lysates were immunoprecipitated with anti-Myc antibody (9E10), with a rabbit polyclonal antibody to p53 (p53fl393), or control IgG serum. The immunocomplexes were examined by Western blot analysis for MDM2 protein (IF2 antibody) or for the Myc-tagged MDMX-(101–490) protein. A portion of each cell lysate (*Input*) was also loaded as a control for expression of MDM2 or the Myc-tagged MDMX-(101–490) protein. *Rxns,* reactions.

null H1299 lung carcinoma cells, and steady-state p53 protein levels were examined by Western blotting. Co-expression of MDM2 with p53 led to a reduction in p53 levels (Fig. 9, *lanes 1* and *2*) as previously observed (17, 18). However, when MDMX was co-expressed with p53 and MDM2, the p53 protein level was restored to a level comparable to that seen in the absence of the transfected MDM2 (Fig. 9*, lane 4*). Notably, the levels of p53 were restored in these triple-transfected cells, even in the presence of quite high levels of MDM2 protein resulting from MDMX binding (Fig. 9, *lane 4*). The data obtained in these experiments, therefore, demonstrate that MDMX blocks MDM2-mediated degradation of p53.

The transfection of cells with a construct expressing MDMX together with p53 reproducibly resulted in a p53 protein level that was actually higher than that detected in the absence of MDMX (Fig. 9, compare *lanes 1* and *3*). This finding indicates that, unlike MDM2, MDMX does not target p53 for degradation; it is also consistent with the idea that MDMX is inhibiting p53 degradation mediated by the endogenous MDM2 protein.

To investigate further the effects of MDMX on this critical MDM2 function, transfection assays were also carried out using the N-terminally truncated MDMX-(101–490) mutant. Since this protein is impaired in its ability to bind p53 directly, any influence it might have on p53 stability would result from its binding to MDM2 or through the recruitment of p53 into a ternary complex. As presented in Fig. 9 (*lane 7*), MDMX-(101–490) also inhibited the MDM2-mediated turnover of p53. Taken

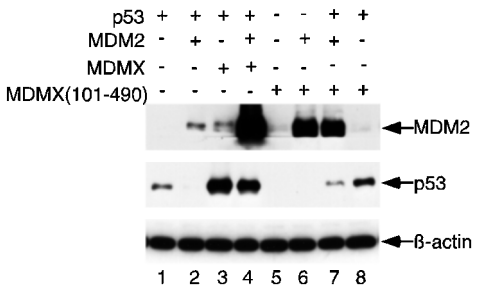

FIG. 9. **MDMX inhibits MDM2-mediated degradation of p53.** H1299 cells were transiently transfected with combinations of expression plasmids encoding MDM2 (1 μg), p53 (0.025 μg), MDMX (5 μg), or Myc-tagged MDMX-(101–490) (5 μg), as indicated. To determine steady-state levels of p53 and MDM2 protein, total cell lysates were subjected to Western blot analysis using anti-p53 monoclonal antibody (DO-1) or anti-MDM2 monoclonal antibody (IF2). Equal loading of cell lysates was confirmed by probing the blot with an anti-β-actin antibody.

together, then, these data support the conclusion that formation of an MDM2-MDMX complex blocks the ability of MDM2 to target p53 for degradation.

DISCUSSION

This investigation was initiated with the goal of identifying interactions between MDM2 and proteins that may be important in influencing its cellular function or expression. The studies described here provide evidence for hetero-oligomerization between MDM2 and MDMX. The interaction of these proteins inhibits the degradation of MDM2, as well as the MDM2-mediated turnover of p53. Thus, MDMX can modulate MDM2 expression and function.

Both MDM2 and MDMX contain C-terminal RING finger motifs. Such domains, which have been defined as a spatially conserved set of cysteine-histidine residues of the type C3HC4, are present in a large and structurally diverse group of proteins (32, 33). Some RING domains seem to provide a surface for protein-protein interactions (32, 33, 40–43). In agreement with this idea, our results indicate that the RING finger domains of MDM2 and MDMX mediate their interaction; an intact RING finger motif within both MDM2 and MDMX is necessary for their association. However, for MDM2 as opposed to MDMX, this domain may not be sufficient; for MDM2 it seems likely that the zinc finger domain also may be required for hetero-oligomerization. Nonetheless, the RING-RING interaction between MDM2 and MDMX provides further evidence that RING domains mediate protein-protein interactions.

Whereas MDM2 and MDMX are structurally related proteins, little is known about the normal cellular functions of the *MDMX* gene. The results of transient transfection assays demonstrate that MDMX proteins can interact with the p53 tumor suppressor protein and inhibit p53 function (34, 35). Unlike *MDM2,* however, the *MDMX* gene is not a transcriptional target of p53. Also, MDM2-deficient mice die early in embryonic development; thus, if *MDMX* is expressed in the early embryo, it cannot functionally compensate for the absence of *MDM2* (44, 45). The current evidence suggests that *MDM2* and *MDMX* serve different physiological functions in the cell and have different regulatory controls.

MDM2, like p53, normally has a short half-life and is degraded by ubiquitin-dependent proteolysis (46, 47). MDM2 control of p53 protein stability involves shuttling it from the nucleus into the cytoplasm, where p53, and probably MDM2, is degraded (48, 49). It has been suggested that MDM2 functions as an E3 ubiquitin ligase for p53, an activity that is lost by mutation of a cysteine residue within the RING domain of MDM2 (19, 20). Furthermore, it is possible that MDM2 itself is a target of its own E3 ligase activity (20). Consistent with this, the ability of MDM2 to target p53 for degradation can be inhibited by mutation of a conserved cysteine residue within the RING finger domain of MDM2 or by truncation of the C terminus containing the RING finger (50).[2] Interestingly, such alterations of the MDM2 protein also result in MDM2 stabilization, in agreement with the suggestion that MDM2 is capable of auto-ubiquitination. This latter finding also suggests that the regulation of MDM2 and p53 stability may be coupled or directly linked (50).

In this study we have obtained additional evidence that the integrity of the C-terminal domain of MDM2 is important in regulating the steady-state levels of MDM2 as well as p53. We have found that binding of MDMX to the C terminus of MDM2 stabilizes the MDM2 protein and also interferes with the degradation of p53. The mechanism by which MDMX modulates MDM2, and p53, stability remains to be defined. MDMX may inhibit MDM2 degradation by blocking a site on MDM2 that is important for E3 ligase function, or for the ability to bind another protein associated with ubiquitin-mediated proteolysis. Alternatively, MDMX might inhibit nucleocytoplasmic shuttling of MDM2, an apparent consequence of the MDM2-$p14^{ARF}$ interaction (30). Because MDM2 and MDMX can interact with each other, and each of these proteins can bind directly to p53, these three proteins may compete with each other for binding. Alternatively, our data indicate that ternary complexes containing all three proteins might also form. In either scenario, however, MDMX has the potential to modulate the expression and biological function of both MDM2 and p53.

An association between MDM2 and MDMX proteins could influence MDM2/p53 expression in a variety of tissues, perhaps affecting cell growth or differentiation pathways. Northern blot analyses indicate that *MDMX* transcripts are expressed at very low levels in most tissues, with relatively higher levels in the thymus (34, 35). Reagents, particularly high quality antibodies, needed to examine MDMX protein expression and function in different cells are just beginning to be developed. Nevertheless, we have been able to demonstrate an interaction of epitope-tagged MDMX with endogenous MDM2 in mammalian cells. Interestingly, our yeast two-hybrid screen for MDM2-interacting proteins was carried out using a human thymus cDNA library, and it led to the isolation of several *MDMX*-derived clones. As suggested by this study, high levels of MDMX protein in a tissue or cell would be expected to interfere with MDM2 turnover, resulting in elevated expression of MDM2 and p53. In a preliminary Western blot analysis to test this possibility, we found that MDM2 and p53 protein levels in the thymus are, in fact, higher than in a number of other tissues examined.[2] Clearly, however, additional studies are needed to test rigorously this hypothesis. A clarification of the interplay among MDM2, MDMX, and p53 should provide a better understanding of the function of these proteins in normal and neoplastic cells.

Acknowledgments—We thank Maureen Murphy for discussion and critical reading of the manuscript and Andre Harris for valuable assistance in the preparation of this manuscript.

REFERENCES

1. Fakharzadeh, S. S., Trusko, S. P., and George, D. L. (1991) *EMBO J.* **10,** 1565–1569
2. Finlay, C. A. (1993) *Mol. Cell. Biol.* **13,** 301–306
3. Cahilly-Snyder, L., Yang-Feng, T., Francke, U., and George, D. L. (1987) *Somatic Cell Mol. Genet.* **13,** 235–244
4. Oliner, J. D., Kinzler, K. W., Meltzer, P. S., George, D. L., and Vogelstein, B. (1992) *Nature* **358,** 80–83
5. Leach, F. S., Tokino, T., Meltzer, P., Burrell, M., Oliner, J. D., Smith, S., Hill, D. E., Sidransky, D., Kinzler, K. W., and Vogelstein, B. (1993) *Cancer Res.* **53,** 2231–2234
6. Cordon-Cardo, C., Latres, E., Drobnjak, M., Oliva, M. R., Pollack, D., Woodruff, J. M., Marechal, V., Chen, J., Brennan, M. F., and Levine, A. J. (1994) *Cancer Res.* **54,** 794–799
7. Momand, J., Jung, D., Wilczynski, S., and Niland, J. (1998) *Nucleic Acids Res.*

26, 3453–3459
8. Landers, J. E., Haines, D. S., Strauss, J. F., III, and George, D. L. (1994) *Oncogene* **9,** 2745–2750
9. Landers, J. E., Cassel, S. L., and George, D. L. (1997) *Cancer Res.* **57,** 3562–3568
10. Capoulade, C., Bressac-de Paillerets, B., Lefrere, I., Ronsin, M., Feunteun, J., Tursz, T., and Wiels, J. (1998) *Oncogene* **16,** 1603–1610
11. Piette, J., Neel, H., and Marechal, V. (1997) *Oncogene* **15,** 1001–1010
12. Freedman, D. A., and Levine, A. J. (1999) *Cancer Res.* **59,** 1–7
13. Momand, J., Zambetti, G. P., Olson, D. C., George, D., and Levine, A. J. (1992) *Cell* **69,** 1237–1245
14. Oliner, J. D., Pietenpol, J. A., Thiagalingam, S., Gyuris, J., Kinzler, K. W., and Vogelstein, B. (1993) *Nature* **362,** 857–860
15. Chen, C. Y., Oliner, J. D., Zhan, Q., Fornace, A. J., Jr., Vogelstein, B., and Kastan, M. B. (1994) *Proc. Natl. Acad. Sci. U. S. A.* **91,** 2684–2688
16. Chen, J., Wu, X., Lin, J., and Levine, A. J. (1996) *Mol. Cell. Biol.* **16,** 2445–2452
17. Haupt, Y., Maya, R., Kazaz, A., and Oren, M. (1997) *Nature* **387,** 296–299
18. Kubbutat, M. H., Jones, S. N., and Vousden, K. H. (1997) *Nature* **387,** 299–303
19. Honda, R., Tanaka, H., and Yasuda, H. (1997) *FEBS Lett.* **420,** 25–27
20. Honda, R., and Yasuda, H. (1999) *EMBO J.* **18,** 22–27
21. Barak, Y., Juven, T., Haffner, R., and Oren, M. (1993) *EMBO J.* **12,** 461–468
22. Juven, T., Barak, Y., Zauberman, A., George, D. L., and Oren, M. (1993) *Oncogene* **8,** 3411–3416
23. Wu, X., Bayle, J. H., Olson, D., and Levine, A. J. (1993) *Genes Dev.* **7,** 1126–1132
24. Zauberman, A., Flusberg, D., Haupt, Y., Barak, Y., and Oren, M. (1995) *Nucleic Acids Res.* **23,** 2584–2592
25. Martin, K., Trouche, D., Hagemeier, C., Sorensen, T. S., La Thangue, N. B., and Kouzarides, T. (1995) *Nature* **375,** 691–694
26. Xiao, Z. X., Chen, J., Levine, A. J., Modjtahedi, N., Xing, J., Sellers, W. R., and Livingston, D. M. (1995) *Nature* **375,** 694–698
27. Grossman, S. R., Perez, M., Kung, A. L., Joseph, M., Mansur, C., Xiao, Z. X., Kumar, S., Howley, P. M., and Livingston, D. M. (1998) *Mol. Cell* **2,** 405–415
28. Pomerantz, J., Schreiber-Agus, N., Liegeois, N. J., Silverman, A., Alland, L., Chin, L., Potes, J., Chen, K., Orlow, I., Lee, H. W., Cordon-Cardo, C., and DePinho, R. A. (1998) *Cell* **92,** 713–723
29. Zhang, Y., Xiong, Y., and Yarbrough, W. G. (1998) *Cell* **92,** 725–734
30. Weber, J. D., Taylor, L. J., Roussel, M. F., Sherr, C. J., and Bar-Sagi, D. (1999) *Nat. Cell Biol.* **1,** 20–26
31. Boddy, M. N., Freemont, P. S., and Borden, K. L. (1994) *Trends Biochem. Sci.* **19,** 198–199
32. Borden, K. L., and Freemont, P. S. (1996) *Curr. Opin. Struct. Biol.* **6,** 395–401
33. Saurin, A. J., Borden, K. L., Boddy, M. N., and Freemont, P. S. (1996) *Trends Biochem. Sci.* **21,** 208–214
34. Shvarts, A., Steegenga, W. T., Riteco, N., van Laar, T., Dekker, P., Bazuine, M., van Ham, R. C., van der Houven van Oordt, W., Hateboer, G., van der Eb, A. J., and Jochemsen, A. G. (1996) *EMBO J.* **15,** 5349–5357
35. Shvarts, A., Bazuine, M., Dekker, P., Ramos, Y. F., Steegenga, W. T., Merckx, G., van Ham, R. C., van der Houven van Oordt, W., van der Eb, A. J., and Jochemsen, A. G. (1997) *Genomics* **43,** 34–42
36. Murphy, M., Pykett, M. J., Harnish, P., Zang, K. D., and George, D. L. (1993) *Cell Growth Differ.* **4,** 715–722
37. Lai, Z., Freedman, D. A., Levine, A. J., and McLendon, G. L. (1998) *Biochemistry* **37,** 17005–17015
38. Olson, D. C., Marechal, V., Momand, J., Chen, J., Romocki, C., and Levine, A. J. (1993) *Oncogene* **8,** 2353–2360
39. Rallapalli, R., Strachan, G., Cho, B., Mercer, W. E., and Hall, D. J. (1999) *J. Biol. Chem.* **274,** 8299–8308
40. Borden, K. L., Boddy, M. N., Lally, J., O'Reilly, N. J., Martin, S., Howe, K., Solomon, E., and Freemont, P. S. (1995) *EMBO J.* **14,** 1532–1541
41. Inouye, C., Dhillon, N., and Thorner, J. (1997) *Science* **278,** 103–106
42. Copps, K., Richman, R., Lyman, L. M., Chang, K. A., Rampersad-Ammons, J., and Kuroda, M. I. (1998) *EMBO J.* **17,** 5409–5417
43. Jensen, D. E., Proctor, M., Marquis, S. T., Gardner, H. P., Ha, S. I., Chodosh, L. A., Ishov, A. M., Tommerup, N., Vissing, H., Sekido, Y., Minna, J., Borodovsky, A., Schultz, D. C., Wilkinson, K. D., Maul, G. G., Barlev, N., Berger, S. L., Prendergast, G. C., and Rauscher, F. J., III (1998) *Oncogene* **16,** 1097–1112
44. Jones, S. N., Roe, A. E., Donehower, L. A., and Bradley, A. (1995) *Nature* **378,** 206–208
45. Montes de Oca Luna, R., Wagner, D. S., and Lozano, G. (1995) *Nature* **378,** 203–206
46. Maki, C. G., Huibregtse, J. M., and Howley, P. M. (1996) *Cancer Res.* **56,** 2649–2654
47. Chang, Y. C., Lee, Y. S., Tejima, T., Tanaka, K., Omura, S., Heintz, N. H., Mitsui, Y., and Magae, J. (1998) *Cell Growth Differ.* **9,** 79–84
48. Freedman, D. A., and Levine, A. J. (1998) *Mol. Cell. Biol.* **18,** 7288–7293
49. Roth, J., Dobbelstein, M., Freedman, D. A., Shenk, T., and Levine, A. J. (1998) *EMBO J.* **17,** 554–564
50. Kubbutat, M. H. G., Ludwig, R. L., Levine, A. J., and Vousden, K. H. (1999) *Cell Growth Differ.* **10,** 87–92